



# Bioinspired Therapeutic Dendrimers as Efficient Peptide Drugs Based on Supramolecular Interactions for Tumor Inhibition\*\*

Xiao Zhang, Zhijun Zhang, Xianghui Xu,\* Yunkun Li, Yachao Li, Yeting Jian, and Zhongwei Gu\*

**Abstract:** Bioinspired tryptophan-rich peptide dendrimers (TRPDs) are designed as a new type of dendritic peptide drugs for efficient tumor therapy. The TRPDs feature a precise molecular structure and excellent water solubility and are obtained in a facile process. Based on the unique features of peptide dendrimers, including highly branched structures, abundant terminal groups, and globular-protein-like architectures, the therapeutic dendrimers show significant supramolecular interactions with DNA through the tryptophan residues (indole rings and amino groups). Further experimental results indicate that TRPDs are efficient antitumor agents both in vitro and in vivo.

Over the past decades, the development of therapeutic agents has played a crucial role to overcome the challenges of disease treatment, particularly in tumor therapy.<sup>[1]</sup> In recent years, more and more drug candidates, including natural products, prodrugs, metal-based drugs, and peptide drugs, have been explored to improve the treatment of various complicated diseases.<sup>[2]</sup> Notably, peptide drugs manifest some advantages as an alternative to therapeutic agents because of their specific bioactivity, high efficacy, and minimal side effects.<sup>[3]</sup> Peptide drugs are inherently multifunctional as they can serve as targeting moieties, immune agents, and tumor inhibitors.<sup>[4]</sup> The bioactivity of peptide drugs largely depends on their amino acid sequences and high-level architectures, and many peptide drugs have achieved satisfactory efficacies both in vitro and in vivo.<sup>[5]</sup> Although more than one hundred peptide drugs have already been introduced to the market, there are still many tough problems to be solved, such as poor solubility, low membrane permeability, and high production costs.<sup>[3b,6]</sup> As a result, novel chemical structures and strategies

are urgently needed to develop versatile peptide drugs for tumor suppression.

On the other hand, dendritic peptides (peptide dendrimers) have several unique features, including monodispersity, a well-defined architecture, and abundant terminal groups, and may be used as nanovehicles for drug delivery.<sup>[7]</sup> Very recently, we took advantage of globular-protein-like peptide dendrimers to build bioinspired virus-mimicking assemblies for the delivery of bioactive molecules.<sup>[8]</sup> More importantly, their highly branched structures have been widely used to develop many vaccines (e.g., glycodendrimers) for immunotherapy.<sup>[9]</sup> However, up to now, only a few examples of dendritic peptide drugs that can exert antitumor activity directly through tailor-made features of the peptide dendrimers have been described.<sup>[3,6]</sup> Therefore, the development of dendritic peptide drugs is of great value for the advancement of peptide drugs and the transformation of dendrimers from nanocarriers into therapeutic agents.

Nature provides numerous natural products, such as doxorubicin and calicheamicin, with antitumor activity, which arises from their remarkable interactions with DNA and their toxicity to tumor cells,<sup>[10]</sup> and also offers a variety of amino acids that interact with DNA, such as tryptophan (Trp).<sup>[11]</sup> At the same time, natural tryptophan-rich peptides (e.g., indolicidin) are used as antimicrobial peptides because of their binding ability to DNA and membranes.<sup>[12]</sup> Therefore, we believed that the development of dendritic peptide drugs for efficient cancer therapy would be valuable and achievable for the following reasons: 1) Their inherent three-dimensional architectures and components mimic natural protein drugs,<sup>[13]</sup> 2) the great number of exposed peripheral residues is expected to strengthen the supramolecular interactions with biomolecules, 3) the surplus terminal groups can be utilized to improve water solubility and association ability, and 4) facile procedures should be applicable for their synthesis and purification. We also hoped that these features would help overcome some drawbacks of current peptide drugs.<sup>[3b]</sup>

Herein, we illustrate the development of a new kind of tryptophan-rich peptide dendrimers (TRPDs), which mimic protein drugs with abundant Trp residues. We investigated the supramolecular interactions between the TRPDs and DNA, intracellular fate, cytotoxicity to several tumor cell lines, and in vivo anticancer activity. Interestingly, we found that supramolecular aggregations with tryptophan residues could reduce the intensity of the fluorescence emission, enhance UV/Vis absorption, and lead to an increase in light scattering.

To confirm our hypothesis, we first designed tryptophan-rich peptide dendrimers with a polyhedral oligomeric silsesquioxane (POSS) core and a lysine backbone using a diver-

[\*] X. Zhang,<sup>[+]</sup> Z. Zhang,<sup>[+]</sup> Dr. X. Xu, Y. Li, Y. Li, Y. Jian, Prof. Z. Gu  
National Engineering Research Center for Biomaterials  
Sichuan University  
Chengdu, Sichuan 610064 (P.R. China)  
E-mail: xianghui.xu@hotmail.com  
zwgu@scu.edu.cn

[+] These authors contributed equally to this work.

[\*\*] This work was supported by the National Natural Science Foundation of China (NSFC, 51133004 and 81361140343), the National Basic Research Program of China (973 program, 2011CB606206), the Joint Sino-German Research Project (GZ756 and GZ905), the Department of Science and Technology of Sichuan Province (2013FZ0003), and the foundation for talent introduction from Sichuan University (YJ201463).

Supporting information for this article is available on the WWW under <http://dx.doi.org/10.1002/anie.201500683>.

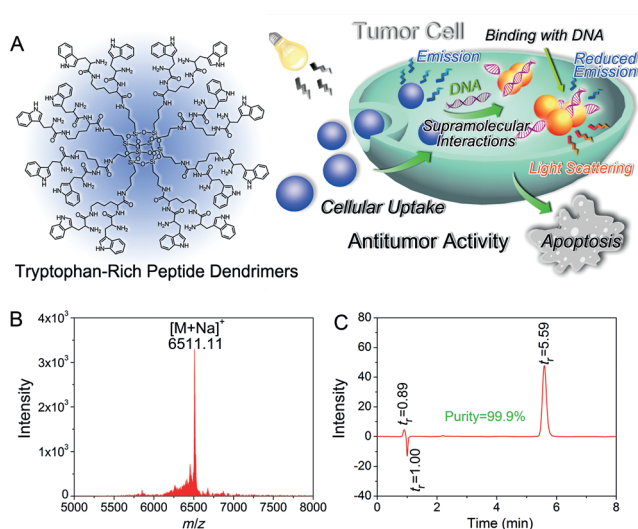


**Figure 1.** A) Chemical structure of the TRPDs and their supramolecular interactions with DNA, which are responsible for their antitumor activity and lead to changes in the fluorescence spectrum. B) MALDI-TOF mass spectrum of the protected TRPDs;  $m/z$ : calcd: 6511.08 ( $[M+Na]^+$ ); found: 6511.11. C) HPLC analysis of the TRPDs; for the conditions see the Supporting Information.

gent synthetic approach. The TRPDs featured many bioactive Trp residues, including sixteen indole rings, which were expected to interact with nucleic acids for an increase in antitumor activity,<sup>[11,12]</sup> and sixteen amino groups, which were incorporated to enhance the water solubility and DNA binding ability (Figure 1 A).<sup>[8]</sup> After accurate synthesis and convenient purification, the molecular weight of the protected TRPDs detected by matrix-assisted laser desorption/ionization time-of-flight mass spectrometry (MALDI-TOF MS,  $M_w = 6511.11$ ) was consistent with the calculated value ( $M_w = 6511.08$ ; Figure 1 B). After deprotection and dialysis, the purity of the TRPDs was determined to be up to 99.9% by HPLC analysis (Figure 1 C; for details on the synthesis and characterization, see the Supporting Information). It is noteworthy that our bioinspired TRPDs were successfully obtained with a controlled molecular structure through a facile synthesis and purification process, which is important for ensuring that the peptide-based agents will be readily available.<sup>[3b,c]</sup>

We then investigated whether the bioinspired tryptophan-rich structure of the dendrimers would lead to significant interactions with DNA. The DNA-binding ability of the TRPDs was determined by an agarose gel retention assay.<sup>[8a]</sup> In Figure 2 A, W/P denotes the molar ratio of Trp (W) moieties contained in the TRPDs to DNA phosphate groups (P). The fluorescence images demonstrate that the DNA mobility (green fluorescence) was completely retarded by the TRPDs (red fluorescence) at a W/P ratio of 10:1. Nevertheless, all contrasted compounds, including individual Trp molecules, G1-Lys (first-generation

lysine-rich dendrimers with sixteen amino groups as part of lysine residues), the Trp/G1-Lys complex, and G2-Lys (second-generation lysine-rich dendrimers with thirty-two amino groups as part of lysine residues), could not bind to DNA at the same amine/phosphate ratio of 10:1 (see the Supporting Information, Figure S15–S18).<sup>[8c]</sup> With an increase in DNA concentration, the zeta potentials of the complexes in aqueous solution were gradually reduced, which also indicated the formation of TRPD/DNA aggregates (Figure 2 B). These results suggest that 1) the dendrimeric structure of the TRPDs strongly amplified the supramolecular interactions of the Trp residues with DNA compared with free Trp and the Trp/G1-Lys complex, and that 2) the indole rings of the Trp residues should play a more important role in DNA binding compared with the positively charged G1-Lys and G2-Lys dendrimers with abundant amino groups.

Fluorescence spectra further corroborated that the dendrimeric structure strengthened the supramolecular interactions between the TRPDs and DNA (Figure 2 C). The fluorescence spectrum of the TRPDs in aqueous medium exhibited a characteristic peak corresponding to the Trp residues at 365 nm (red line). Upon the addition of DNA to the TRPD solution, the fluorescence emission at 365 nm decreased in intensity owing to the binding of the indole rings to DNA, while a peak that is due to light scattering appeared at 578 nm owing to the formation of TRPD/DNA aggregates.<sup>[14]</sup> However, both an individual Trp molecule and the Trp/G1-Lys complex caused neither fluorescence quenching of the chromophores nor light scattering (Figures S20 and

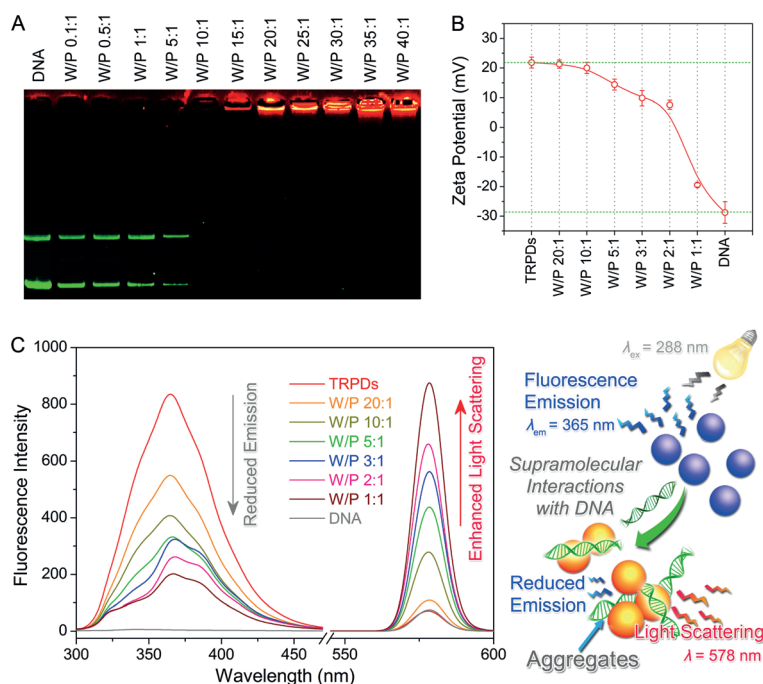


**Figure 2.** A) Merged fluorescence images of the TRPDs (red fluorescence) with DNA (green fluorescence) in a gel electrophoresis assay with W/P ratios from 0.1:1 to 40:1. B) Zeta potentials of the TRPDs, DNA, and their complexes at the same TRPD concentration ( $5 \mu\text{g mL}^{-1}$ ) in aqueous solution at  $25^\circ\text{C}$  (mean  $\pm$  standard deviation,  $n = 3$ ). C) Fluorescence emission spectra of the TRPD/DNA aggregates and light scattering at W/P ratios of 20:1 to 1:1 at a TRPD concentration of  $5 \mu\text{g mL}^{-1}$  in aqueous solution. Excitation wavelength: 288 nm.

S21). Furthermore, other natural nucleic acids (e.g., a DNA sodium salt from salmon testes) were also able to induce significant fluorescence quenching and light scattering owing to the formation of the TRPD-based aggregates (Figure S24). Therefore, it became evident that both the indole rings of the Trp residues and the dendrimeric structure are crucial for the strong supramolecular interactions of the bioinspired TRPDs with DNA.

To explore the supramolecular interactions between TRPDs and DNA in detail, a series of studies were carried out. First, transmission electron microscopy (TEM) and scanning electron microscopy (SEM) images showed the nanostructures of the TRPD/DNA aggregates (Figure 3A; see also Figure S25). Subsequently, it was found that the absorption peaks at approximately 250–300 nm in the UV/Vis spectra became stronger and broader, which was ascribed to the  $\pi$  interactions within the TRPD/DNA aggregates (Figure 3B).<sup>[15]</sup> One- and two-dimensional NMR spectra recorded the signal changes of the indole rings that were caused by  $\pi$  interactions (Figure 3C; see also Figure S27). When the DNA concentration was increased,  $^1\text{H}$  NMR spectroscopy (600 MHz) revealed that the signals corresponding to the indole rings at 6.0–7.5 ppm gradually shifted to higher frequencies and became broader and indistinct, which is due to charge transfer between the indole rings and DNA.<sup>[16]</sup> An inspection of the FTIR spectra provided further evidence of significant interactions in the TRPD/DNA aggregates (Figure 3D). For example, the guanine bands of DNA at

1698  $\text{cm}^{-1}$  shifted towards a lower frequency at 1675  $\text{cm}^{-1}$  at a W/P ratio of 10:1; meanwhile, the band at 1088  $\text{cm}^{-1}$  ( $\text{PO}_2$  symmetric) shifted to 1016  $\text{cm}^{-1}$ .<sup>[17]</sup> To elucidate the supramolecular interactions between the indole rings and DNA more clearly, we synthesized dendrimers that are rich in indole rings, but do not feature any peripheral amino groups, which had very poor water solubility (Figure S28). These dendrimers also induced fluorescence quenching, increased light scattering, and enhanced absorption, which indicates the presence of  $\pi$ -interactions between DNA and the indole rings. Taken together, we concluded that the exposed amino groups improved the water solubility of the therapeutic TRPDs through synergetic electrostatic interactions, and that the indole rings efficiently interacted with DNA and disturbed the DNA structure through strong  $\pi$  interactions.

Next, we investigated whether the TRPDs could serve as therapeutic agents for efficient tumor inhibition *in vitro*. As shown in Figure 4A, the therapeutic TRPDs showed distinct cytotoxicity towards 4T1, HepG2, HeLa, MCF-7, and SKOV3 tumor cell lines when administered at a wide range of concentrations. Moreover, the TRPDs still displayed remarkable antitumor effects against drug-resistant cell lines, including MCF-7/ADR and SKOV3/ADR. Even at a low TRPD concentration (10  $\mu\text{g mL}^{-1}$ ), the dendrimers could induce more than 50 % inhibition of the 4T1, SKOV3, and SKOV3/ADR cell lines. The corresponding cell states of the tumor cell lines were studied by inverted optical microscopy (see the Supporting Information). However, individual Trp molecules,

G1-Lys, and the Trp/G1-Lys complex were not found to display cytotoxicity towards these tumor cell lines even at a relative high concentration (100  $\mu\text{g mL}^{-1}$ ; Figure 4B). Furthermore, highly positively charged G2-Lys also showed no cytotoxicity towards these tumor cell lines at the same concentration. Amino acids usually have good biocompatibility because amino acids, such as the above-mentioned Trp and Lys, are indispensable components of organisms. The biological activities of the peptide drugs were regulated by their amino acid sequence and high-level architecture. For example, the cytotoxicity of the TRPDs was ascribed to amplification effects induced by their tryptophan-rich dendrimeric structures, which tremendously enhanced the supramolecular interactions between the Trp residues and DNA to achieve tumor suppression.

Next, the cellular uptake of the TRPDs and their intracellular interactions with DNA were studied by confocal laser scanning microscopy (CLSM) using the 4T1 tumor cell line. After incubation with TRPDs for two hours, two different fluorescence emissions were detected by CLSM (Figure 5A). According to the fluorescence emission spectra, the blue fluorescence at low wavelengths (400–500 nm) was emitted by internalized free TRPDs, and the scattering of red light at high wavelengths (550–800 nm) was attributed to TRPD/DNA aggre-

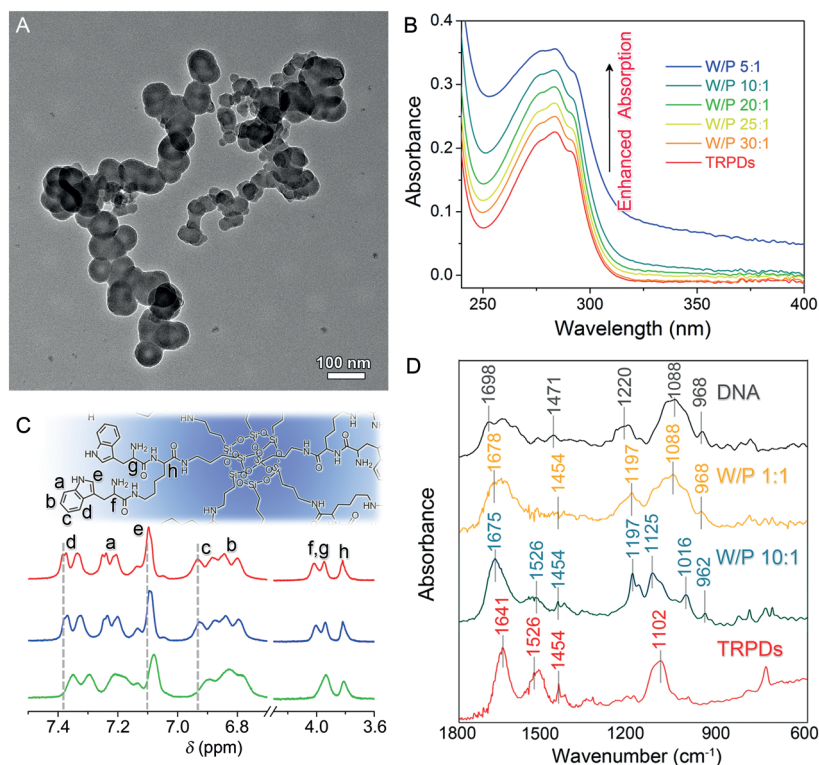


**Figure 3.** A) TEM image of the TRPD/DNA aggregates at a W/P ratio of 10:1. B) UV/Vis spectra of the TRPDs and the TRPD/DNA aggregates at different W/P ratios in aqueous media at a TRPD concentration of 10  $\mu\text{g mL}^{-1}$ . C)  $^1\text{H}$  NMR spectra of the TRPDs (red line) and the TRPD/DNA complexes (W/P=100:1: blue line; W/P=25:1: green line). D) FTIR spectra of DNA, TRPDs, and their aggregates at different W/P ratios.



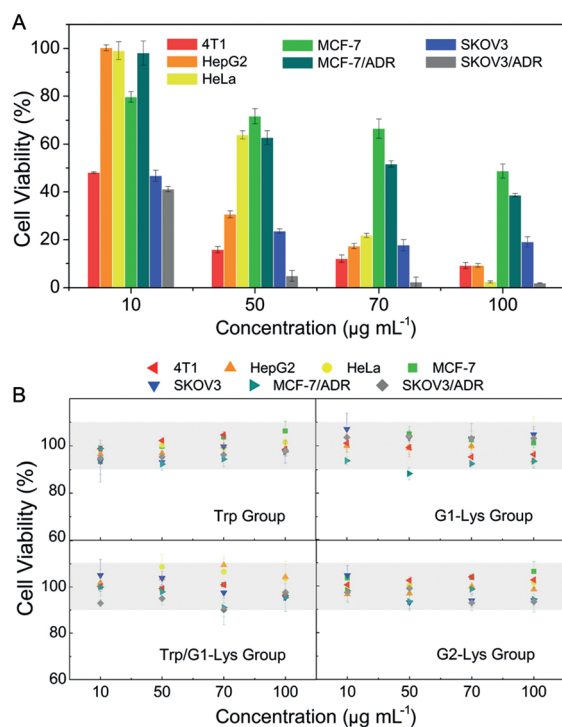


**Figure 4.** A) Cytotoxicity of the TRPDs towards 4T1, HepG2, HeLa, MCF-7, MCF-7/ADR, SKOV3, and SKOV3/ADR tumor cell lines at various concentrations. B) Cell viabilities of several cell lines after exposure to Trp, G1-Lys, the Trp/G1-Lys complex, and G2-Lys for 24 hours; gray areas correspond to a cell viability of 90–110%.

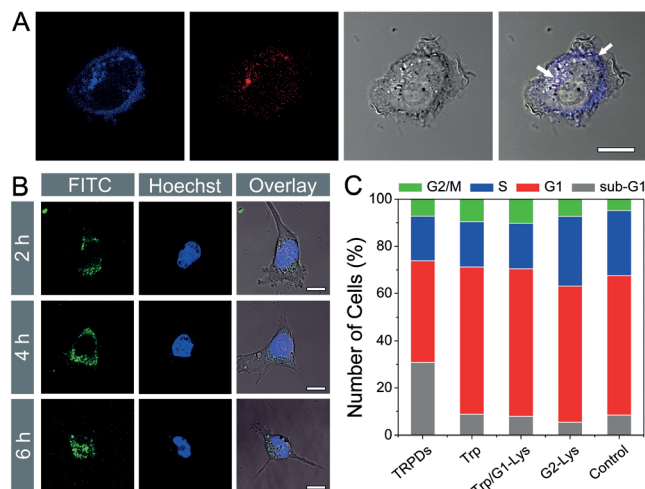


**Figure 5.** A) CLSM images of 4T1 cells incubated with TRPDs for two hours; the fluorescence emission of the TRPDs was detected by the blue channel and light scattering by the red channel. B) CLSM images for the intracellular tracking of TRPDs at different time points; the FITC-labeled TRPDs were observed by the green channel and nuclei stained with Hoechst 33342 by the blue channel; merged images are also shown. C) Cell cycle distribution of 4T1 cells after incubation with TRPDs, Trp, the Trp/G1-Lys complex, and G2-Lys for 24 hours. All scale bars: 10 µm.

gates. To further study cellular uptake and intracellular binding with DNA, the peripheral amino groups of the TRPDs were labeled with commercial fluorescein isothiocyanate (FITC), and intercellular DNA was stained with

Hoechst 33342 (Figure 5B). After exposure to FITC-labeled TRPDs, the TRPDs were quickly internalized into 4T1 tumor cells and effectively dispersed in the cytoplasm within two hours. When the incubation time was increased to four hours, the TRPDs were found to be mainly scattered across the perinuclear region and bound to DNA in the cytoplasm (overlap of green and blue fluorescence). Encouragingly, some TRPDs had been transported into the nuclei after six hours, allowing for sufficient interactions with nuclear DNA. Similar results were obtained with the HepG2 tumor cell line (Figure S35). These results demonstrate that transmembrane transport of the TRPDs was efficiently realized, and that they interacted with intracellular DNA.

Cell-cycle analysis was used to test whether cytokinesis arrest was disturbed by the TRPDs. It is known that the sub-G1 phase is an important indicator of cell apoptosis.<sup>[18]</sup> After incubation with TRPDs at a low concentration of 10 µg mL<sup>-1</sup> for 24 hours, approximately 30% of the 4T1 cell population was apoptotic (gray color, Figure 5C). The number of apoptotic cells in the presence of the TRPDs was three times larger than in the blank control group (ca. 10% of the 4T1 cells in the sub-G1 phase). Compared with the blank control group, no obvious changes in cytokinesis arrest and apoptosis were observed after exposure to Trp molecules, the Trp/G1-Lys complex, and G2-Lys. Staining with propidium iodide (PI) revealed that the number of apoptotic cells was much larger when treated with TRPDs than in the control groups (Figure S36). Collectively, the TRPDs could be quickly internalized into cells and caused apoptosis, thus exerting considerable cytotoxicity towards tumor cell lines.

To explore the *in vivo* antitumor efficacy of the TRPDs, BALB/c mice bearing a 4T1 tumor were used as animal models through intratumoral injections. Histological and immunohistochemical studies were carried out to determine the *in vivo* therapeutic efficacy of the TRPDs (Figure 6A).<sup>[19]</sup> Haematoxylin and eosin (H&E) staining of tumor slices showed that the administration of TRPDs (4 doses of 5 mg TRPDs per kg of body weight) resulted in a marked damage of tumor tissues after treatment over 21 days, substantially differing from the compact and superabundant tumor cells in the tumor tissues of mice that were administered with phosphate-buffered saline (PBS). More importantly, the administration of TRPDs more efficiently inhibited CD31-positive vessel formation and reduced the proliferation of Ki-67 positive tumor cells compared with other control groups. Meanwhile, the administration of TRPDs led to a significantly greater number of apoptotic cells (TUNEL-positive cells) in the tumor tissues after treatment. The semiquantitative results of the immunohistochemical studies also confirmed that these TRPDs could provide considerable *in vivo* anti-tumor efficacy (Figure 6B). For the major organs (heart, liver, spleen, lung, and kidney), no distinct histopathologic abnormalities were observed in the TRPD-administered group using microscopic examinations; moreover, the high antitumor activity of the TRPDs greatly suppressed tumor metastasis to other tissues and organs, especially in the lung (Figure S39).<sup>[20]</sup>

In summary, bioinspired tryptophan-rich peptide dendrimers have been shown to be a promising novel type of



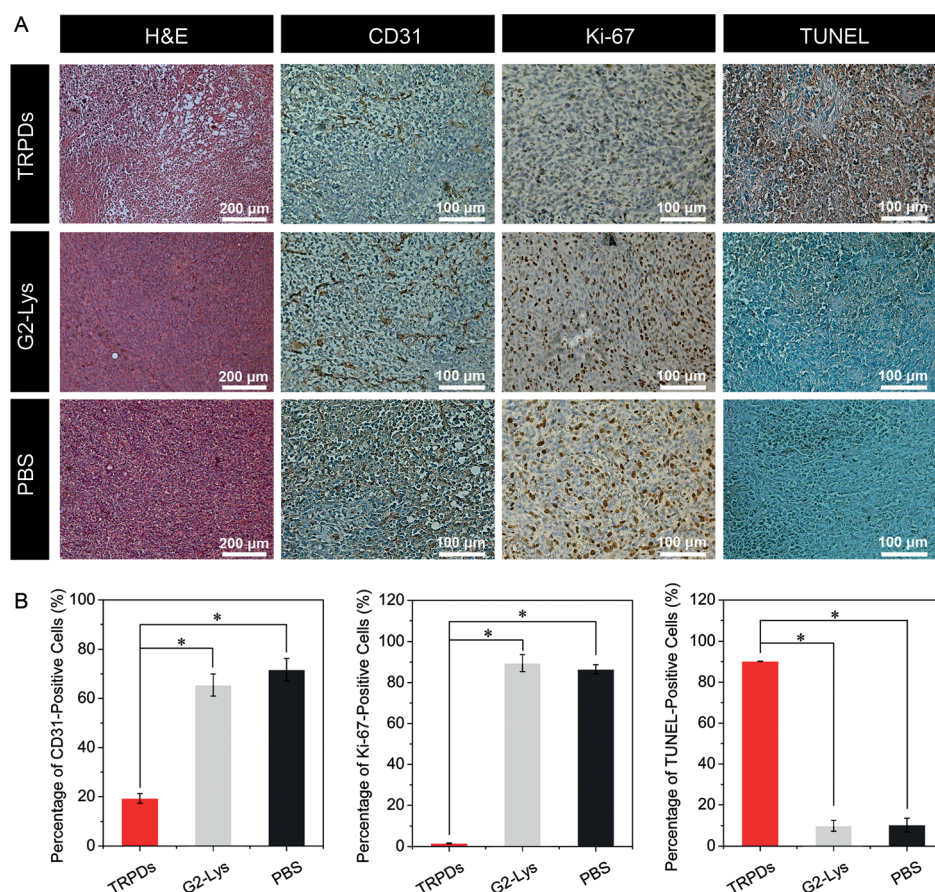


**Figure 6.** A) Histological and immunohistochemical images of the H&E, CD31, Ki-67, and TUNEL assays for tumor tissues after treatment with different doses over 21 days. CD31-positive vessels, Ki-67-positive cells, and TUNEL-positive cells are stained brown. B) Semiquantitative analysis of the immunohistochemical studies of CD31-positive vessels, Ki-67-positive cells, and TUNEL-positive cells in tumor tissue (mean  $\pm$  standard deviation,  $n=3$ ,  $*p<0.001$ ).

peptide drug candidates for tumor therapy. These dendritic peptide drugs feature a precise molecular structure and excellent water solubility and were obtained through a facile process. As expected, the tryptophan-rich dendrimeric structures facilitate significant supramolecular interactions between the indole rings and DNA, which leads to the formation of supramolecular aggregates. Most importantly, the therapeutic TRPDs have a high membrane permeability, significantly disturb the cell cycle, and display superior cytotoxicity towards various tumor cell lines. The TRPDs inhibited the proliferation of tumor cells in vivo and accelerated cell apoptosis at tumor sites. Next, we aim to endow the therapeutic dendrimers with tumor-specific toxicity through an in-depth study, for example, by targeted modification and tumor-activation strategies. We hope that this work will set the stage for the development of efficient peptide drugs and therapeutic dendrimers.

**Keywords:** antitumor agents · dendrimers · peptide drugs · supramolecular chemistry · tryptophan

**How to cite:** *Angew. Chem. Int. Ed.* **2015**, *54*, 4289–4294  
*Angew. Chem.* **2015**, *127*, 4363–4368

- [1] a) L. S. Goupil, J. H. McKerrrow, *Chem. Rev.* **2014**, *114*, 11131–11137; b) G. M. Keserü, G. M. Makara, *Nat. Rev. Drug Discovery* **2009**, *8*, 203–212.
- [2] a) L. Du, A. J. Robles, J. B. King, D. R. Powell, A. N. Miller, S. L. Mooberry, R. H. Cichewicz, *Angew. Chem. Int. Ed.* **2014**, *53*, 804–809; *Angew. Chem.* **2014**, *126*, 823–828; b) D. Ghislieri, A. P. Green, M. Pontini, S. C. Willies, I. Rowles, A. Frank, G. Grogan, N. J. Turner, *J. Am. Chem. Soc.* **2013**, *135*, 10863–10869; c) S. Jang, S. Hyun, S. Kim, S. Lee, I.-S. Lee, M. Baba, Y. Lee, J. Yu, *Angew. Chem. Int. Ed.* **2014**, *53*, 10086–10089; *Angew. Chem.* **2014**, *126*, 10250–10253; d) D. Y. Q. Wong, C. H. F. Yeo, W. H. Ang, *Angew. Chem. Int. Ed.* **2014**, *53*, 6752–6756; *Angew. Chem.* **2014**, *126*, 6870–6874; e) Z. Zhou, X. Ma, C. J. Murphy, E. Jin, Q. Sun, Y. Shen, E. A. Van Kirk, W. J. Murdoch, *Angew. Chem. Int. Ed.* **2014**, *53*, 10949–10955; *Angew. Chem.* **2014**, *126*, 11129–11135.
- [3] a) C. Borghouts, C. Kunz, B. Groner, *J. Pept. Sci.* **2005**, *11*, 713–726; b) D. J. Craik, D. P. Fairlie, S. Liras, D. Price, *Chem. Biol. Drug Des.* **2013**, *81*, 136–147; c) P. Vlieghe, V. Lisowski, J. Martinez, M. Khrestchatsky, *Drug Discovery Today* **2010**, *15*, 40–56.
- [4] a) H. Cai, M.-S. Chen, Z.-Y. Sun, Y.-F. Zhao, H. Kunz, Y.-M. Li, *Angew. Chem. Int. Ed.* **2013**, *52*, 6106–6110; *Angew. Chem.* **2013**, *125*, 6222–6226; b) O. Pando, S. Stark, A. Denkert, A. Porzel, R. Preusentanz, L. A. Wessjohann, *J. Am. Chem. Soc.* **2011**, *133*, 7692–7695; c) E. Ruoslahti, *Adv. Mater.* **2012**, *24*, 3747–3756.
- [5] a) S. A. Sievers, J. Karanicolas, H. W. Chang, A. Zhao, L. Jiang, O. Zirafi, J. T. Stevens, J. Münch, D. Baker, D. Eisenberg, *Nature* **2011**, *475*, 96–100; b) J. Hu, C. Chen, S. Zhang, X. Zhao, H. Xu, X. Zhao, J. R. Lu, *Biomacromolecules* **2011**, *12*, 3839–3843; c) M. Stach, T. N. Siriwardena, T. Köhler, C. van Delden, T. Darbre, J. L. Reymond, *Angew. Chem. Int. Ed.* **2014**, *53*, 12827–12831; *Angew. Chem.* **2014**, *126*, 13041–13045.
- [6] L. Otvos Jr., in *Peptide-Based Drug Design*, Vol. 494 (Ed.: L. Otvos), Humana Press, Totowa, NJ, **2008**, pp. 1–8.
- [7] a) L. Crespo, G. Sanclimens, M. Pons, E. Giralt, M. Royo, F. Albericio, *Chem. Rev.* **2005**, *105*, 1663–1682; b) T. Darbre, J.-L. Reymond, *Acc. Chem. Res.* **2006**, *39*, 925–934; c) J. Lazniewska, K. Milowska, T. Gabrylak, *Wiley Interdiscip. Rev. Nanomed. Nanobiotechnol.* **2012**, *4*, 469–491.
- [8] a) X. Xu, Y. Jian, Y. Li, X. Zhang, Z. Tu, Z. Gu, *ACS Nano* **2014**, *8*, 9255–9264; b) X. Xu, Y. Li, H. Li, R. Liu, M. Sheng, B. He, Z. Gu, *Small* **2014**, *10*, 1133–1140; c) X. Xu, H. Yuan, J. Chang, B. He, Z. Gu, *Angew. Chem. Int. Ed.* **2012**, *51*, 3130–3133; *Angew. Chem.* **2012**, *124*, 3184–3187.
- [9] T. C. Shiao, R. Roy, *New J. Chem.* **2012**, *36*, 324–339.

- [10] a) G. M. Cragg, P. G. Grothaus, D. J. Newman, *Chem. Rev.* **2009**, *109*, 3012–3043; b) F. E. Koehn, G. T. Carter, *Nat. Rev. Drug Discovery* **2005**, *4*, 206–220.
- [11] a) T. Montenay-Garestier, C. Helene, *Nature* **1968**, *217*, 844–845; b) T. Behmoaras, J.-J. Toulme, C. Helene, *Nature* **1981**, *292*, 858–859; c) P. Saikumar, R. Murali, E. P. Reddy, *Proc. Natl. Acad. Sci. USA* **1990**, *87*, 8452–8456.
- [12] a) R. L. Alfred, N. M. Shagaghi, E. A. Palombo, M. Bhave, *Microbial pathogens and strategies for combating them: science, technology and education*, Formatex Research Center, Badajoz, Spain, **2013**; b) C.-H. Hsu, C. Chen, M.-L. Jou, A. Y.-L. Lee, Y.-C. Lin, Y.-P. Yu, W.-T. Huang, S.-H. Wu, *Nucleic Acids Res.* **2005**, *33*, 4053–4064.
- [13] S. Svenson, D. A. Tomalia, *Adv. Drug Delivery Rev.* **2012**, *64*, 102–115.
- [14] a) R. F. Pasternack, C. Bustamante, P. J. Collings, A. Giannetto, E. J. Gibbs, *J. Am. Chem. Soc.* **1993**, *115*, 5393–5399; b) R. F. Pasternack, P. J. Collings, *Science* **1995**, *269*, 935–939; c) J. G. McAfee, S. P. Edmondson, I. Zegar, J. W. Shriver, *Biochemistry* **1996**, *35*, 4034–4045.
- [15] a) M. I. Khamis, J. Casas-Finet, A. Maki, *J. Biol. Chem.* **1987**, *262*, 1725–1733; b) C. R. Martinez, B. L. Iverson, *Chem. Sci.* **2012**, *3*, 2191–2201; c) S. Tashiro, M. Tominaga, M. Kawano, B. Therrien, T. Ozeki, M. Fujita, *J. Am. Chem. Soc.* **2005**, *127*, 4546–4547.
- [16] a) K. Wüthrich, *Angew. Chem. Int. Ed.* **2003**, *42*, 3340–3363; *Angew. Chem.* **2003**, *115*, 3462–3486; b) M. Avinash, T. Govindaraju, *Nanoscale* **2011**, *3*, 2536–2543.
- [17] a) D. Agudelo, P. Bourassa, G. Bérubé, H.-A. Tajmir-Riahi, *Int. J. Biol. Macromol.* **2014**, *66*, 144–150; b) S. Nafisi, A. A. Saboury, N. Keramat, J.-F. Neault, H.-A. Tajmir-Riahi, *J. Mol. Struct.* **2007**, *827*, 35–43.
- [18] S. W. Fesik, *Nat. Rev. Cancer* **2005**, *5*, 876–885.
- [19] a) A. I. Minchinton, I. F. Tannock, *Nat. Rev. Cancer* **2006**, *6*, 583–592; b) A. Ventura, D. G. Kirsch, M. E. McLaughlin, D. A. Tuveson, J. Grimm, L. Lintault, J. Newman, E. E. Reczek, R. Weissleder, T. Jacks, *Nature* **2007**, *445*, 661–665.
- [20] a) I. J. Fidler, *Nat. Rev. Cancer* **2003**, *3*, 453–458; b) J. Xiao, X. Duan, Q. Yin, Z. Zhang, H. Yu, Y. Li, *Biomaterials* **2013**, *34*, 9648–9656.

Received: January 24, 2015

Published online: February 26, 2015